

Implementation and Analysis of Physiologically Based Pharmacokinetic (PBPK) Model for Docetaxel in Cancer Chemotherapy

Md. Zahidul Islam and M. S. Alam

Department of Electrical & Electronic Engineering, University of Dhaka, Dhaka-1000, Bangladesh

E-mail: zahidul@du.ac.bd, msalam@du.ac.bd

Received on 19.10.17. Accepted for publication on 08.08.18

ABSTRACT

Physiologically based pharmacokinetic (PBPK) models represent an important class of dosimetry models that are useful for predicting internal dose at target organs in human body. In this paper, a whole body Docetaxel based PBPK model has been implemented and analyzed. This model shows the variations and distributions of drug concentrations over time at different organs of human body. Higher drug concentration can affect human body with different toxic side effect. This model can help clinicians to measure the concentration of drugs at different organs using computer based simulation and to decide the correct dose for a patient.

Keywords: Mathematical Model of Human Body, Docetaxel, Drug Concentration, Physiologically based Pharmacokinetic (PBPK) Model.

1. Introduction

Computational systems biology is an emerging field that bridges mathematics, computer science and engineering and applies these tools to problems in the clinical setting. Currently, there exists an array of mathematical models to capture patient and disease dynamics and to predict future growth and prognosis. The knowledge of the anatomy and physiology of the studied species is employed to develop a pharmacokinetic (PK) model that accurately describes plasma, tissue, and in some cases, tumor concentrations, following drug delivery. Physiologically based pharmacokinetic (PBPK) modeling is a mathematical modeling technique for predicting the absorption, distribution, metabolism and excretion of synthetic or natural chemical substances in humans and other animal species. PBPK modeling is used in pharmaceutical research, drug development and in health risk assessment for cosmetics or general chemicals [1]. It is usually multi-compartmental model with compartments corresponding to predefined organs or tissues with interconnections corresponding to blood or lymph flows. A system of differential equations for concentration or quantity of substance on each compartment can be written, and its parameters represent blood flows, pulmonary ventilation rate, organ volumes etc [1].

In this paper, a whole body Docetaxel based PBPK model proposed by Florian in 2008 [2] has been implemented and analyzed. Docetaxel is an anti-mitotic chemotherapeutic drug that interferes with cell division by binding to tubulin in the M-phase of cell growth [3]. Breast, ovarian, and prostate cancers are treated with Docetaxel as a mono-agent [3,4], and it is combined with platinum-based chemotherapy (e.g., cisplatin) or cisplatin and 5-fluorouracil (5-FU) to treat non-small-cell lung cancer [5] and head-and-neck cancer [6]. The PBPK model shows the output drug concentration at different organs of human body and its variations with time [2,6].

2. Physiologically Based Pharmacokinetic (PBPK) Model for Docetaxel

A PBPK model was developed by Florian and co-workers in 2008 [2] to represent different tissues or organs in the body which is known as Physiologically Based Pharmacokinetic model for Docetaxel(Doc). The model not only captures Doc plasma concentration, but also captures tissue concentrations and bound/unbound drug amounts with intracellular tissue in each tissue compartment. The system-wide distribution of Doc was described using a PBPK model, as shown in Figure 1 [2].

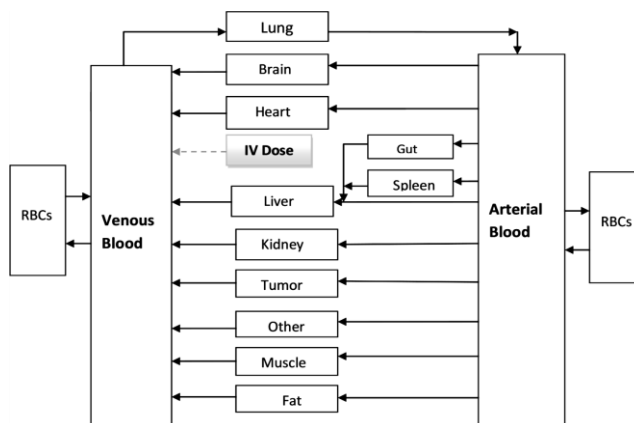


Fig. 1: PBPK model for the distribution of doc in plasma, various tissues, and subcutaneously implemented tumor xenografts.

In PBPK model the whole body was divided into some compartments or different organs of human body. These organs in human body were then represented by some differential equations, which were developed depending on the response, characteristics, behavior and practical data for different organs. Drug administration is included in the model as an infusion into the venous compartment, which subsequently distributes throughout the rest of the body [2]. In equation 1 $u(t)$ is the input drug schedule. The complete sets of equations for the Docetaxel human PBPK model are listed in following section [2, 6, 8].

Venous Blood:

$$\frac{dC_v}{dt} = \frac{1}{(1-f_{hem})} (F_{in}C_{in} - F_{tot}C_{ven}) + \frac{f_{hem}}{(1-f_{hem})} k_{rbcp} C_{rbcv} - k_{plsrbc} f_{unb} C_{ven} + \frac{u(t)}{V_{ven}(1-f_{hem})} \quad (1)$$

$$\frac{dC_{rbcv}}{dt} = -k_{rbcp} C_{rbcv} + \frac{(1-f_{hem})}{f_{hem}} k_{plsrbc} f_{unb} C_{ven} \quad (2)$$

Lung:

$$\frac{dC_{lv}}{dt} = \frac{F_{tot}}{V_{lv}} (C_{ven} - C_{lv}) - k_{lve} f_{unb} C_{lv} + \frac{V_{le}}{V_{lv}} k_{lev} C_{le} \quad (3)$$

$$\frac{dC_{le}}{dt} = \frac{V_{le}}{V_{lv}} k_{lve} f_{unb} C_{lv} - k_{lev} C_{le} + k_{bind_{out}} C_{lb} - k_{bind_{in}} C_{le} \quad (4)$$

$$\frac{dC_{lb}}{dt} = -k_{bind_{out}} C_{lb} + k_{bind_{in}} C_{le} \quad (5)$$

Arterial Blood:

$$\frac{dC_{art}}{dt} = \frac{1}{V_{art}(1-f_{hem})} (F_{tot}C_{lv} - F_{tot}C_{art}) + \frac{f_{hem}}{(1-f_{hem})} k_{rbcp} C_{rbca} - k_{plsrbc} f_{unb} C_{art} \quad (6)$$

$$\frac{dC_{rbca}}{dt} = k_{rbcp} C_{rbca} + \frac{(1-f_{hem})}{f_{hem}} k_{plsrbc} f_{unb} C_{art} \quad (7)$$

Gut:

$$\frac{dC_{gv}}{dt} = \frac{F_g}{V_{gv}} (C_{art} - C_{gv}) \quad (8)$$

Brain:

$$\frac{dC_{bv}}{dt} = \frac{F_b}{V_{bv}} (C_{art} - C_{bv}) - k_{bve} f_{unb} C_{bv} + \frac{V_{be}}{V_{bv}} k_{bev} C_{be} \quad (9)$$

$$\frac{dC_{be}}{dt} = \frac{V_{bv}}{V_{be}} k_{bve} f_{unb} C_{bv} - k_{lev} C_{be} + k_{bind_{out}} C_{bb} - k_{bind_{in}} C_{be} \quad (10)$$

$$\frac{dC_{bb}}{dt} = -k_{bind_{out}} C_{bb} + k_{bind_{in}} C_{be} \quad (11)$$

Spleen:

$$\frac{dC_{sv}}{dt} = \frac{F_s}{V_{sv}} (C_{art} - C_{sv}) - k_{sve} f_{unb} C_{sv} + \frac{V_{se}}{V_{sv}} k_{sev} C_{se} \quad (12)$$

$$\frac{dC_{se}}{dt} = \frac{V_{sv}}{V_{se}} k_{sve} f_{unb} C_{sv} - k_{sev} C_{se} + k_{bind_{out}} C_{sb} - k_{bind_{in}} C_{se} \quad (13)$$

$$\frac{dC_{sb}}{dt} = -k_{bind_{out}} C_{sb} + k_{bind_{in}} C_{se} \quad (14)$$

Liver:

$$\frac{dC_{liv}}{dt} = \frac{1}{V_{liv}} (F_{li}C_{art} + F_gV_{gv} + F_sC_{sv} - (F_g + F_s + F_{li})C_{liv}) - k_{live} f_{unb} C_{liv} + \frac{V_{lie}}{V_{liv}} k_{liev} C_{lie} \quad (15)$$

$$\frac{dC_{kv}}{dt} = \frac{V_{liv}}{V_{lie}} k_{live} f_{unb} C_{liv} - k_{liev} C_{lie} + k_{bind_{out}} C_{lib} - k_{bind_{in}} C_{lie} - k_{ctli} C_{lie} \quad (16)$$

$$\frac{dC_{lib}}{dt} = -k_{bind_{out}} C_{lib} - k_{bind_{in}} C_{lie} \quad (17)$$

Kidney:

$$\frac{dC_{kv}}{dt} = \frac{F_k}{V_{kv}} (C_{art} - C_{kv}) - k_{kve} f_{unb} C_{kv} + \frac{V_{ke}}{V_{kv}} k_{kev} C_{ke} \quad (18)$$

$$\frac{dC_{ke}}{dt} = \frac{V_{kv}}{V_{ke}} k_{kve} f_{unb} C_{kv} - k_{kev} C_{ke} + k_{bind_{out}} C_{kb} - k_{bind_{in}} C_{ke} \quad (19)$$

$$\frac{dC_{kb}}{dt} = -k_{bind_{out}} C_{kb} + k_{bind_{in}} C_{ke} \quad (20)$$

Muscle:

$$\frac{dC_{mv}}{dt} = \frac{F_m}{V_{mv}} (C_{art} - C_{mv}) - k_{mve} f_{unb} C_{mv} + \frac{V_{me}}{V_{mv}} k_{mev} C_{me} \quad (21)$$

$$\frac{dC_{me}}{dt} = \frac{V_{mv}}{V_{me}} k_{mve} f_{unb} C_{mv} - k_{mev} C_{me} + k_{bind_{out}} C_{mb} - k_{bind_{in}} C_{me} \quad (22)$$

$$\frac{dC_{mb}}{dt} = -k_{bind_{out}} C_{mb} + k_{bind_{in}} C_{me} \quad (23)$$

Fat:

$$\frac{dC_{fv}}{dt} = \frac{F_f}{V_{fv}} (C_{art} - C_{fv}) - k_{fve} f_{unb} C_{fv} + \frac{V_{fe}}{V_{fv}} k_{fev} C_{fe} \quad (24)$$

$$\frac{dC_{fe}}{dt} = \frac{V_{fv}}{V_{fe}} k_{fve} f_{unb} C_{fv} - k_{fev} C_{fe} + k_{bind_{out}} C_{fb} - k_{bind_{in}} C_{fe} \quad (25)$$

$$\frac{dC_{fb}}{dt} = -k_{bind_{out}} C_{fb} + k_{bind_{in}} C_{fe} \quad (26)$$

Tumor:

$$\frac{dC_{tv}}{dt} = \frac{F_t}{V_{tv}} (C_{art} - C_{tv}) - k_{tve} f_{unb} C_{tv} + \frac{V_{te}}{V_{tv}} k_{tev} C_{te} \quad (27)$$

$$\frac{dC_{te}}{dt} = \frac{V_{tv}}{V_{te}} k_{tve} f_{unb} C_{tv} - k_{tev} C_{te} + k_{bind_{out}} C_{tb} - k_{bind_{in}} C_{te} \quad (28)$$

$$\frac{dC_{tb}}{dt} = -k_{bind_{out}} C_{tb} + k_{bind_{in}} C_{te} \quad (29)$$

Heart:

$$\frac{dC_{hv}}{dt} = \frac{F_h}{V_{hv}} (C_{art} - C_{hv}) - k_{hve} f_{unb} C_{hv} + \frac{V_{he}}{V_{hv}} k_{hev} C_{he} \quad (30)$$

$$\frac{dC_{he}}{dt} = \frac{V_{hv}}{V_{he}} k_{hve} f_{unb} C_{hv} - k_{hev} C_{he} + k_{bind_{out}} C_{hb} - k_{bind_{in}} C_{he} \quad (31)$$

$$\frac{dC_{hb}}{dt} = -k_{bind_{out}} C_{hb} + k_{bind_{in}} C_{he} \quad (32)$$

Others:

$$\frac{dC_{ov}}{dt} = \frac{F_o}{V_{ov}} (C_{art} - C_{ov}) - k_{ove} f_{unb} C_{ov} + \frac{V_{oe}}{V_{ov}} k_{oev} C_{oe} \quad (33)$$

$$\frac{dC_{oe}}{dt} = \frac{V_{ov}}{V_{oe}} k_{ove} f_{unb} C_{ov} - k_{oev} C_{oe} + k_{bind_{out}} C_{ob} - k_{bind_{in}} C_{oe} \quad (34)$$

$$\frac{dC_{ob}}{dt} = -k_{bind_{out}} C_{ob} + k_{bind_{in}} C_{oe} \quad (35)$$

Parameter Estimation

The above equations represent sets of equations for Docetaxel PBPK model [2]. Where, C_i is the drug concentration in tissue i , F_{in} is the blood flow rate into tissue i , V_i is the volume of tissue i , and C_{in} is the inlet drug concentration for tissue i , which comes from: (i) the venous blood supply in the case of the lungs; (ii) from the spleen, gut, and arterial compartment for the liver; or (iii) from the arterial compartment for all other body tissues [2]. Diffusion-limited tissues have both a vascular (v) and extra-vascular tissue (e) space (volumes V_{iv} and V_{ie} , respectively), with separate concentrations, C_{iv} and C_{ie} , intra-tissue transfer rates, k_{ive} and k_{iev} , f_{unb} is the unbound drug fraction, C_{ib} is the drug concentration in the additional "bound" subcompartment, $k_{bind_{out}}$ and $k_{bind_{in}}$ are retention

rates within the tissue, k_{cli} is the rate of drug clearance from the liver, C_{ven} and C_{rbc} are the concentrations in venous plasma and circulating red blood cells respectively, f_{hem} is the hematocrit fraction [2]. The parameters for the human PBPK model used in this paper are taken from literature as reported in [2, 6].

3. Implementation of PBPK Model for Docetaxel

Docetaxel PBPK model has been implemented here using SIMULINK®[9]. Differential equations contains different parameters, these are represented by different blocks in Simulink as shown in the figure 2. In this analysis different drug schedules has been used as an input to check the drug concentration variation & distribution over time for different organs. The details of block by block implementation for Arterial blood has been shown in the

following Simulink figure, and in this way different compartments are implemented using different blocks and connected each others. For the implementation of this model Simulink Continuous block, Math operations block,

Sources block, Sinks blocks are used. One block is connected to another using connector to get the Simulink model shown below.

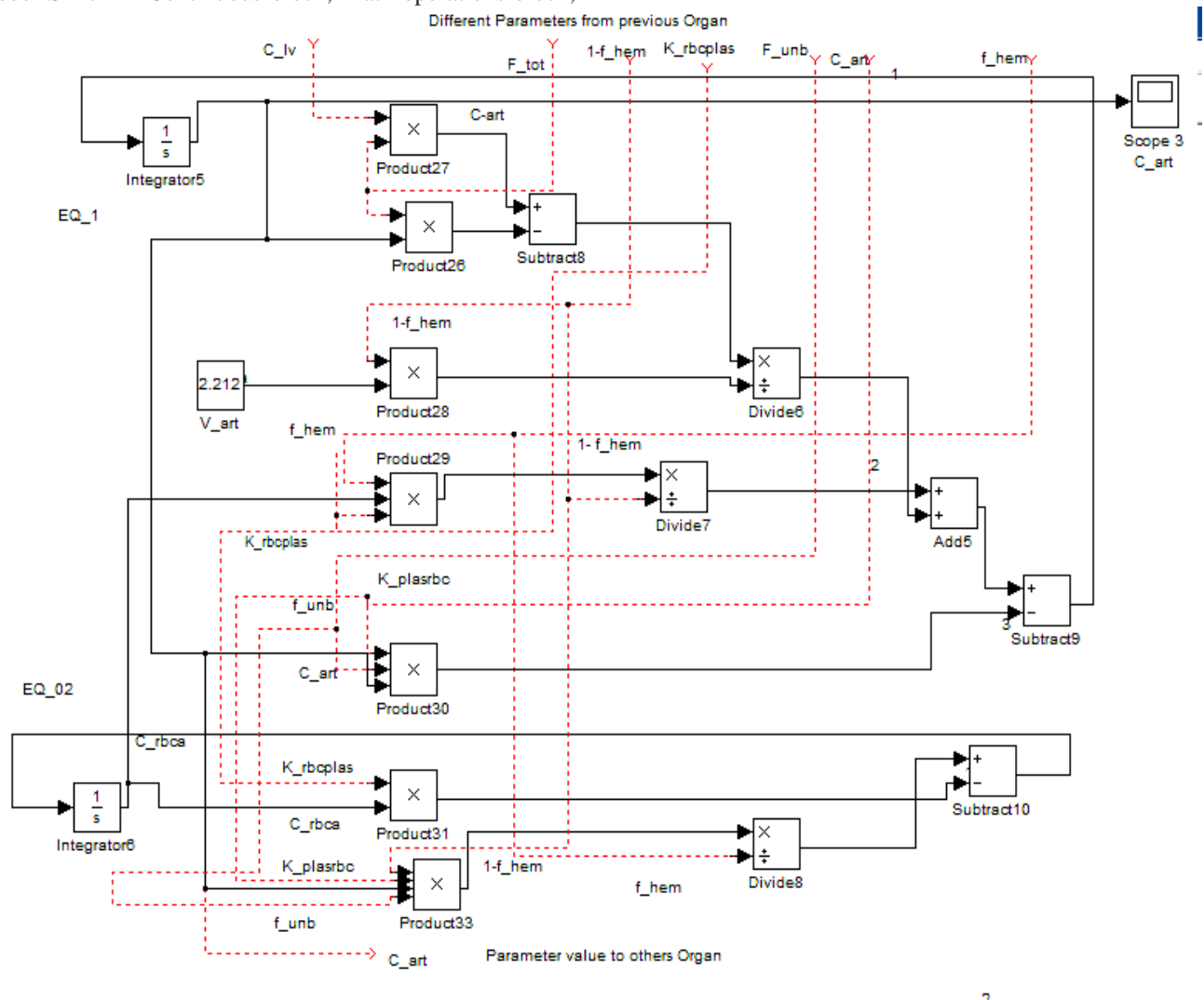


Fig. 2: Implementation of differential equation for Arterial Blood

4. Results and Analysis of PBPK Model

For PBPK model analysis some input dose schedules $u(t)$ has been used in the first equation (Equation 1). For different dose schedule the output concentration of Docetaxel at different organs of human body are shown below. To study the response of PBPK model, we used a drug schedule which

is shown in Figure 3 and designed for 260 days. The maximum drug concentration is 33 and minimum concentration is about 7. Here this drug schedule $u(t)$ was generated by “Signal Builder” using SIMULINK®[9]. This schedule shows that drugs are continuous and drug concentration level changing at different time interval.

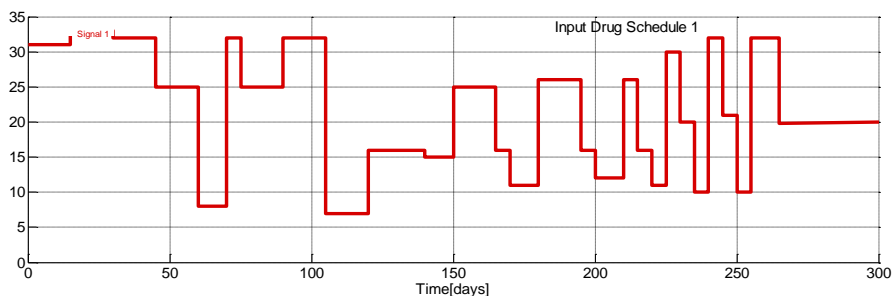


Fig. 3: Input Dose schedule-1

For the above input dose schedule to the PBPK model, different organs of human body react in different manner. The output drug concentration distribution varies over time in the case of different organs. The resultant variation of the drug (Docetaxel) concentration has been shown in Figure 4 to Figure 13.

The input drug schedule was designed for 260 days, but we observed the variations of drug concentration for different organs for only 2 days, because the drug concentration will become constant after 2 or 3 days. The variation of Docetaxel concentration for RBC has been shown in Figure 4. Figure 5 and 6 shows the variation of measured drug concentration for lung and brain. The rate of reduction of doc concentration for lung is lower than that in brain but higher than that in spleen. The output Docetaxel concentrations for other organs for input dose-1 schedule are shown in Figure 7 to 13.

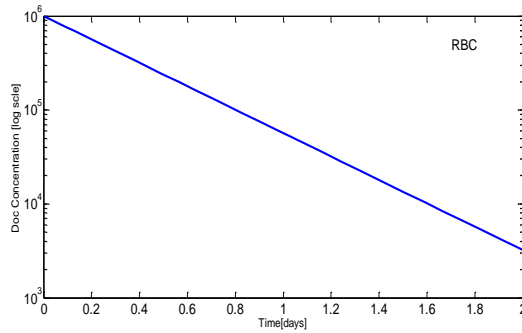


Fig. 4: Measured Doc concentration versus time data in human for RBC (Dose -1)

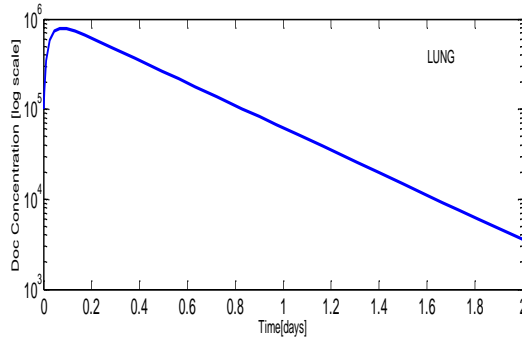


Fig. 5: Measured Doc concentration versus time data in human for Lung (Dose -1)

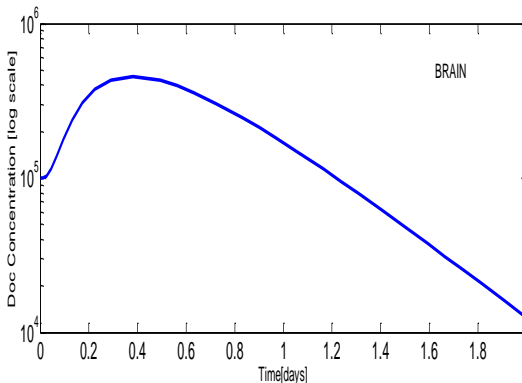


Fig. 6: Measured Doc concentration versus time data in human for Brain (Dose -1)

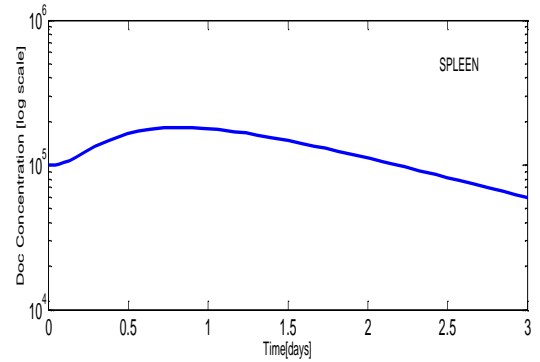


Fig. 7: Measured Doc concentration versus time data in human for Spleen (Dose -1)

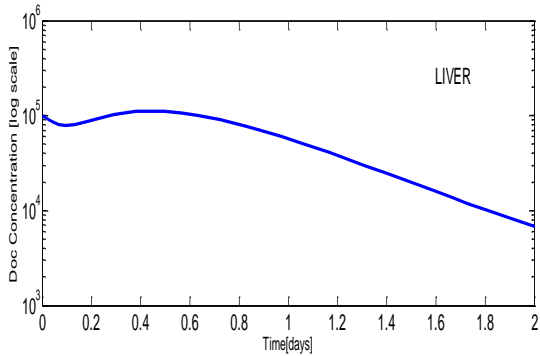


Fig. 8: Measured Doc concentration versus time data in human for Liver (Dose -1)

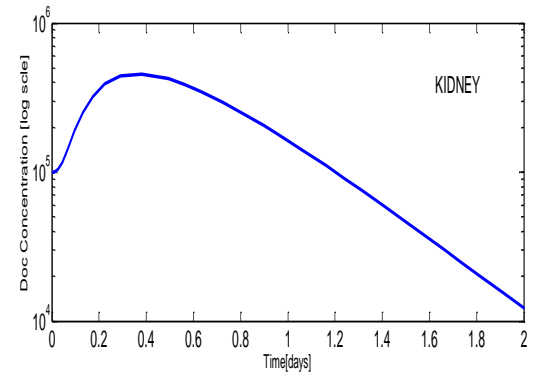


Fig. 9: Measured Doc concentration versus time data in human for Kidney (Dose -1)

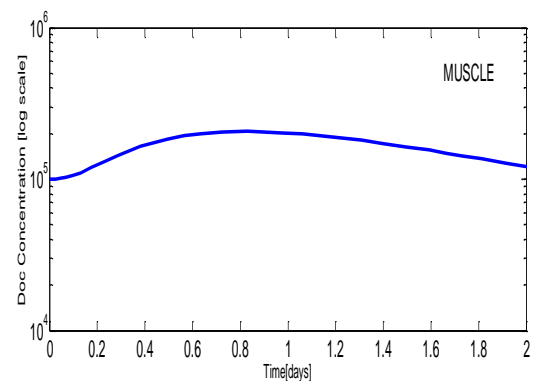


Fig. 10: Measured Doc concentration versus time data in human for Muscle (Dose -1)

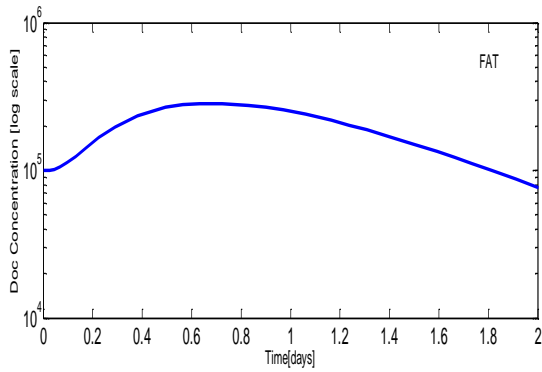


Fig. 11: Measured Doc concentration versus time data in human for Fat (Dose -1)

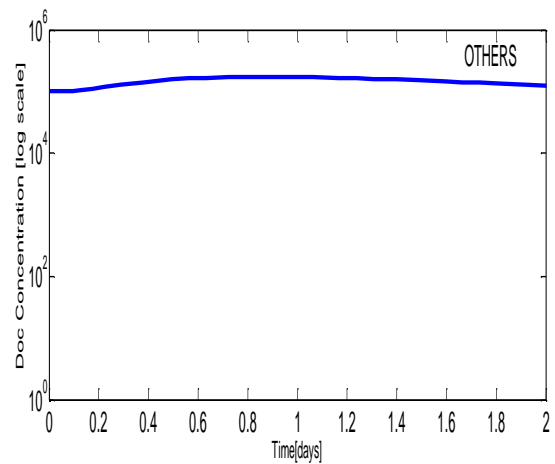


Fig. 13: Measured Doc concentration versus time data in human for Others (Dose -1)

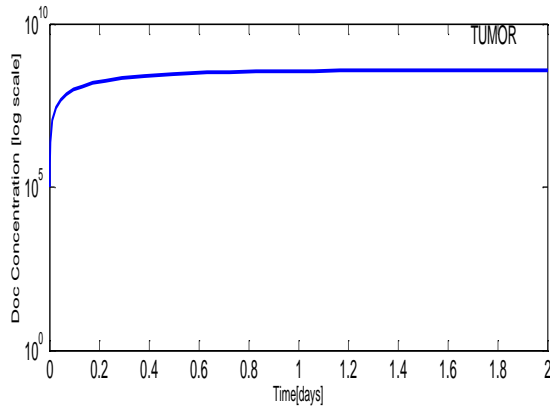


Fig. 12: Measured Doc concentration versus time data in human for Tumor (Dose -1)

A second dose schedule-2 has been used and shown in Figure 14 which is also built by us using Matlab Signal builder. Maximum level of input drug is 50 and minimum level is 0.

This dose schedule has been designed for 50 days. On the first day the input drug level is 50 but from day 2 to 9 its level is zero and input becomes 50 at day 10 and so on. For input dose schedule-2 the response from PBPK model has been shown in Figure 15 to Figure 24.

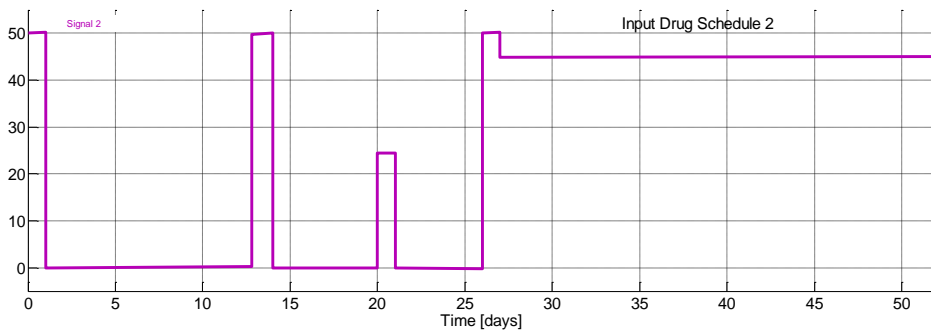


Fig. 14: Input dose schedule-2

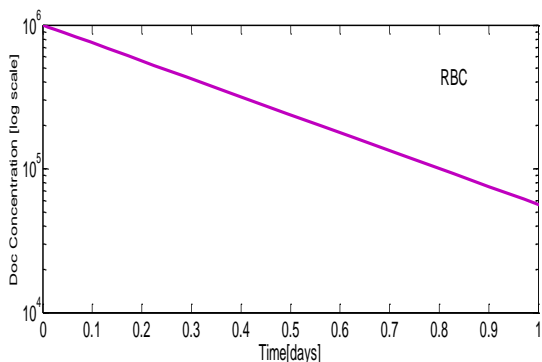


Fig. 15: Measured Doc concentration versus time data in human for RBC (Dose-2)

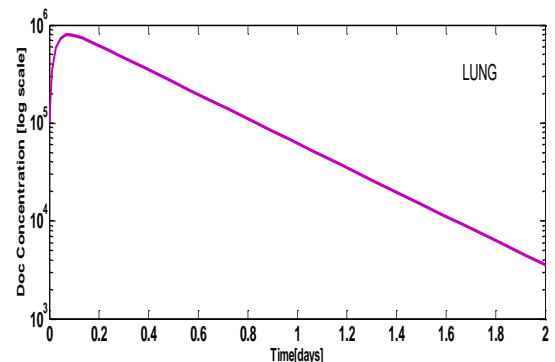


Fig. 16: Measured Doc concentration versus time data in human for Lung (Dose-2)

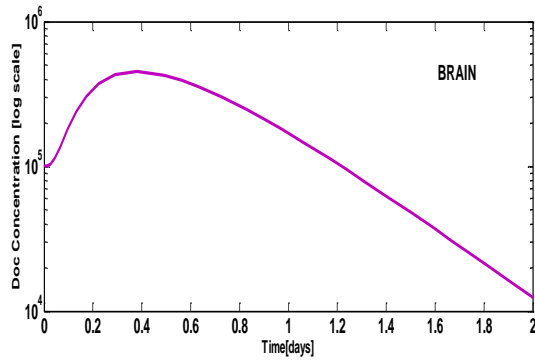


Fig. 17: Measured Doc concentration versus time data in human for Brain (Dose-2)

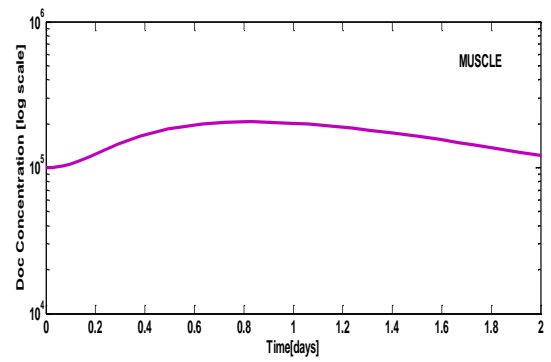


Fig. 21: Measured Doc concentration versus time data in human for Muscle (Dose-2)

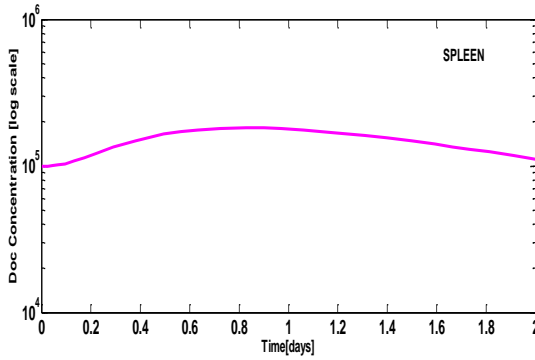


Fig. 18: Measured Doc concentration versus time data in human for Spleen (Dose-2)

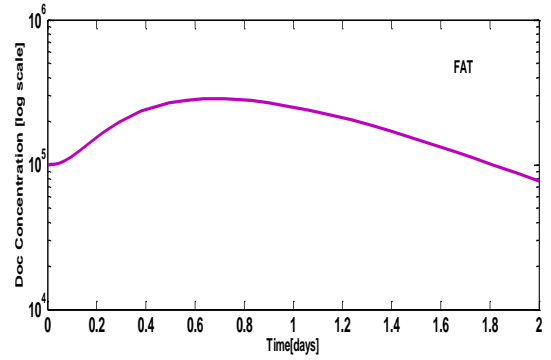


Fig. 22: Measured Doc concentration versus time data in human for Fat (Dose-2)

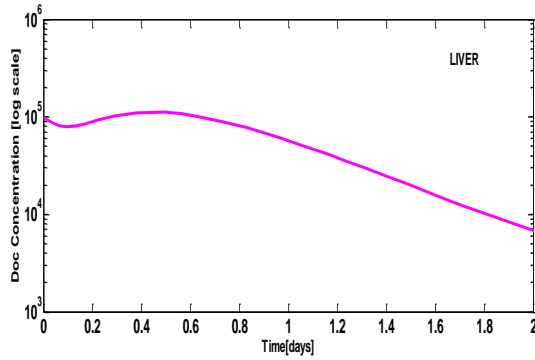


Fig. 19: Measured Doc concentration versus time data in human for Liver (Dose-2)

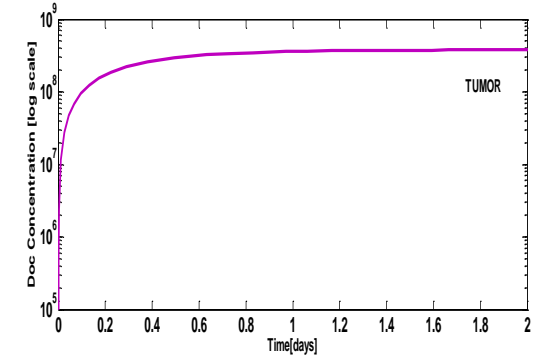


Fig. 23: Measured Doc concentration versus time data in human for Tumor (Dose-2)

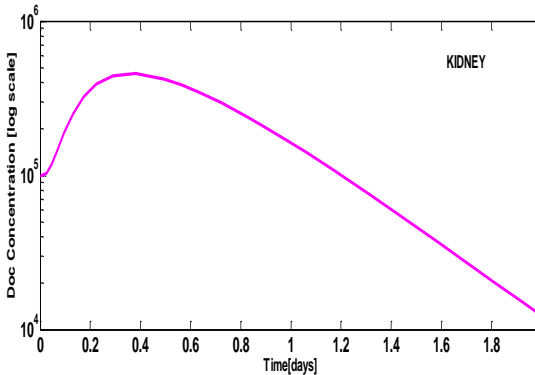


Fig. 20: Measured Doc concentration versus time data in human for Kidney (Dose-2)

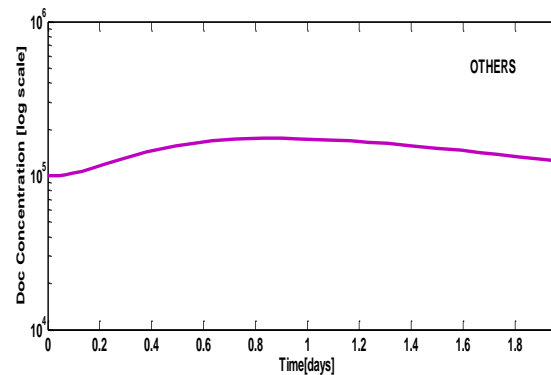


Fig. 24: Measured Doc concentration versus time data in human for Others (Dose-2)

5. Conclusions

PBPK model can describe plasma, tissue, and in some cases, tumor concentrations, following drug delivery. It can capture patient and disease dynamics and predict growth of cancer tumor as well. This paper focused on the implementation of PBPK model using Simulink and observation of drug concentration variation and distribution throughout the whole body over time for different input dose.

For the input dose 1 and input dose 2, output drug concentrations have been measured for different organs from the PBPK model which were shown in the previous figure. In this analysis two different types of dose schedule have been used, and the most important observation is noted that the output drug concentration has remained approximately similar for all kinds of input dose schedule. The maximum level of output drug concentration in different organs of a human body is approximately 10^5 [2]. But the drug concentration decreased within a few days and it remains at a fixed level after 3 or 4 days. Therefore the result has been shown in the analysis only for two or three days. Input output drug relationship is quite different for tumor, and output drug concentration for tumor remains at a large and constant level.

Thus this paper has represented an important simulation and analysis for different organs in human body and shown the interaction of different organs with input drugs. Different organs interact with drugs in different manner. But each and every organ in human body has a maximum acceptable level of drugs. If the drug concentration exceeds that limit then it causes various dangerous toxic side effects on body. Clinicians can observe the drug concentration using Docetaxel Based whole body PBPK model for better understanding of drug-body interactions.

References

1. http://en.wikipedia.org/wiki/Physiologically_based_pharmacokinetic_modelling (Last accessed on March 15, 2014)
2. J.A. Florian. "Modeling and dose schedule design for cyclic-specific chemotherapeutics", PhD Dissertation, University of Pittsburgh, 2008.
3. Crown, J. (2001). Docetaxel: overview of an active drug for breast cancer. *The Oncologist*, 6(Supplement 3), pp. 1-4.
4. Shepherd, F. A., Dancey, J., Ramlau, R., Mattson, K., Gralla, R., O'Rourke, M. and Berille, J. (2000). Prospective randomized trial of docetaxel versus best supportive care in patients with non-small-cell lung cancer previously treated with platinum-based chemotherapy. *Journal of Clinical Oncology*, 18(10), pp. 2095-2103.
5. Fossella, F., Pereira, J. R., von Pawel, J., Pluzanska, A., Gorbounova, V., Kaukel, E. and Belani, C. P. (2003). Randomized, multinational, phase III study of docetaxel plus platinum combinations versus vinorelbine plus cisplatin for advanced non-small-cell lung cancer: The TAX 326 study group. *Journal of Clinical Oncology*, 21(16), pp. 3016-3024.
6. Thang Ho. "A model based clinically-relevant chemotherapy scheduling algorithm for anticancer agents", PhD Dissertation, University of Pittsburg, 2014.
7. Nestorov, I. (2003). Whole body pharmacokinetic models. *Clinical pharmacokinetics*, 42(10), pp. 883-908.
8. Godfrey K., "Compartmental models and their application", New York: Academic Press, 1983.
9. MATLAB Reference Guide, The Math Works, Inc., 2015